Results in Engineering 22 (2024) 102262

Contents lists available at ScienceDirect

Results in Engineering

journal homepage: www.sciencedirect.com/journal/results-in-engineering

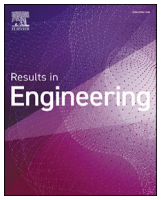

Research paper

Stability analysis for an *ad-hoc* model predictive control in DC/DC converters with a constant power load

Alejandro Garcés-Ruiz [a,*], Walter Gil-González [a], Oscar Danilo Montoya [b]

[a] Department of Electrical Engineering, Faculty of Engineering, Universidad Tecnológica de Pereira, Pereira 660003, Colombia
[b] Grupo de Compatibilidad e Interferencia Electromagnética, Facultad de Ingeniería, Universidad Distrital Francisco José de Caldas, Bogotá 110231, Colombia

ARTICLE INFO

Keywords:
One-step model predictive control
Second-order DC/DC converters
Discrete bi-linear model
Asymptotic stability

ABSTRACT

This paper presents a stability analysis for a horizon-one continuous control set model predictive control (MPC) for DC/DC converters connected to a constant power loads (CPLs). Different MPC approaches have been previously presented, each tailored to a specific type of converter but without a formal stability proof, failing to ensure robust performance across various operating conditions. Unlike previous works in the scientific literature, our approach is general and applicable to any second-order DC/DC converter, including the Buck, Boost, Buck-Boost, and non-inverting Buck-Boost converters. A formal stability analysis was conducted using the proposed approach, initially for the open-loop system and subsequently for the closed-loop system. The trace-determinant or triangle criterion was employed for discrete-time systems in $\mathbb{R}^2$. Three analyses were conducted to evaluate the performance of the proposed MPC, showing the stability issues of DC/DC converters with CPLs in open loops. This work proposes solutions using the suggested technique. Numerical simulations utilizing the Boost and Buck-Boost converters demonstrate that, in open-loop operation, even minor perturbations in the CPL value can destabilize the behavior of electrical variables. In addition, simulations show that, for the Boost converter, the settling time was about 1.5 *ms*. Meanwhile, in the Buck-Boost case, it was about 5 *ms*. Standardized control indicators, such as the integral absolute error criterion (IAE), the integral of the time-multiplied absolute error criterion (ITAE), and the integral of the time-multiplied square error criterion (ITSE), confirm the effective performance of the proposed one-step MPC. The values range between 1.521×10^{-2} and 4.591×10^{-6} for the Boost converter, and between 6.607×10^{-3} and 3.366×10^{-6} for the Buck-Boost topology.

1. Introduction

Policies concerning the quality of the electricity service stipulate that the operation of all devices connected to the system must adhere to certain minimum standards, including appropriate voltage levels, minimal harmonic distortion, satisfactory power factor values, and minimal frequency deviations [1,2]. These policies are fundamental in active distribution networks, where the number of active power components is on the rise with the advancements made in power electronic conversion systems for integrating energy storage technologies, renewable energy systems, and power loads with special requirements [3]. Power electronic converter topologies enable the integration of all these elements into AC or DC distribution networks by employing appropriate and robust control methodologies [4], which play a crucial role in complying with power quality policies [5].

Optimal control theory constitutes an important research area in power electronics applications [6], and it is well-known and robust for linear and nonlinear systems [7]. In power electronic conversion and its applications, model predictive control (MPC) has garnered significant attention in industrial settings due to its simplicity, its high performance, and its ability to effectively incorporate constraints in complex and nonlinear dynamic systems [8].

In general, MPC is a strategy that utilizes a dynamic system model to predict future behavior and optimize control actions accordingly, often considering constraints on inputs and outputs [9]. This optimization process is typically performed over a finite time horizon, updating control actions at each time step based on the latest measurements and

Abbreviations: CPL, Constant power load; CCS-MPC, Continuous control set model predictive control; FCS-MPC, Finite control set model predictive control; MPC, Model predictive control; OCP, Optimal control problem.

* Corresponding author.
E-mail addresses: alejandro.garces@utp.edu.co (A. Garcés-Ruiz), wjgil@utp.edu.co (W. Gil-González), odmontoyag@udistrital.edu.co (O.D. Montoya).

https://doi.org/10.1016/j.rineng.2024.102262
Received 4 March 2024; Received in revised form 18 April 2024; Accepted 11 May 2024
Available online 16 May 2024

predictions [10]. MPC has been extensively studied and applied in various fields, including process control [11], automotive systems [12], mechanical systems [13], robotics [14,15], power systems [16], and power electronics [17,18]. The main idea behind MPC is to solve an optimal control problem (OCP) for real-time applications.

The use of MPC theory for power electronics and power systems applications has the following advantages. (i) MPC can anticipate future system performance, allowing to adjust control inputs accordingly. This allows for quick responses to disturbances such as load changes or sudden voltage variations. Essentially, this capability enhances transient performance, ensuring that the converter reacts appropriately to dynamic conditions [19]. (ii) MPC theory enables the handling of multiple constraints (*e.g.*, current and voltage limitations) and complex dynamical models while ensuring an optimal system operation under various conditions. Its adaptable nature allows defining specific performance objectives such as output regulation or efficiency maximization, making it a suitable control methodology for power electronic converter applications [20].

The disadvantages of using MPC theory in power converters can be summarized in two main aspects. (i) Firstly, it entails processing time complexity, as it is dependent on the optimization equivalent problem and the number of time windows analyzed, which can lead to delays and increased hardware requirements in physical implementations [21]. Secondly, (ii) it is dependent on an effective model representation, as inaccurate models can lead to sub-optimal control performance or even instability in some particular applications [22]. Considering the above, these works outline the rationale for employing a one-step MPC approach in DC-DC converter applications.

In MPC, stability is ensured by using long horizons or including additional stability constraints into the OCP [23]. However, practical power electronics applications necessitate an optimization problem formulation that is computationally tractable. Hence, long horizons or complicated constraints may be impracticable, even with recent advances in micro-controller technology. As a direct consequence, in power electronics applications, MPC is usually performed in short horizons (usually one step ahead), with stability remaining an open question in the scientific literature.

On the other hand, the growing need for cleaner, more environmentally friendly, and efficient energy systems has led to the rise of DC microgrids, a viable option to meet all requirements from the production and distribution of decentralized energy to its use. These microgrids use DC for both transmission and distribution, unlike their AC counterparts. This shift towards DC technology offers several advantages, including reduced energy losses, enhanced renewable energy sources integration, and improved compatibility with DC loads, *e.g.*, electronic devices. In DC microgrids and power distribution systems, DC/DC converters have become essential building blocks [24,25]. These converters require more sophisticated controls to adapt to their new context [26]. It is important to understand that the loads present in DC microgrids play a crucial role in their effective design and control. These loads can be broadly classified into linear and non-linear based on their behavior with regard to the relationship between voltage and current. Linear loads do not pose a challenge from a control perspective because they maintain a proportional relationship between voltage and current [27]. Some linear loads that can be found in a DC micro-grid include incandescent lamps and heating elements (resistive loads). In contrast, non-linear loads do not adhere to Ohm's Law and exhibit a non-linear relationship between voltage and current. Among these, constant power loads (CPLs) are particularly noteworthy: they exhibit an inverse relationship between current and voltage, introducing negative resistive effects into the system [28]. This unique characteristic causes general stability issues in DC microgrids [29,30].

Two MPC approaches are commonly implemented in power electronics applications [31]. The first approach is known as finite control set MPC (FCS-MPC), which leverages the finite switching state in the converter to select the state that minimizes the cost function [32]. FCS-MPC operates at a variable frequency, leading to increased losses and making it difficult to calibrate output filters [33]. In some cases, FCS-MPC requires oversizing some parameters for proper operation. Additionally, it requires that micro-controllers constantly perform calculations to evaluate all possible solutions. The second approach is continuous control set MPC (CCS-MPC), which operates with a constant switching frequency through pulse-width modulation (PWM) [34].

A study into the effectiveness of FCS-MPC and CCS-MPC in regulating the speed of an induction motor was conducted in [34]. This work revealed that CCS-MPC requires less computational effort and provides less ripple in stator currents, leading to lower losses. In addition, enhanced performance has been demonstrated across various applications, including permanent magnet synchronous generators [35], six-phase drivers [36], DC/AC converters [37], and matrix converters [38]. In contrast, there is a noticeable lack of literature on the application of CCS-MPC in the field of DC/DC converters, with only a few articles available [39]. Recently, a one-step CCS-MPC was proposed to regulate the output voltage of second-order DC/DC converters [40], utilizing an incremental model to design the control. This incremental model is only applicable for linear loads, *e.g.*, resistances). However, DC microgrids may also include CPLs, which are nonlinear. Therefore, a formal control design with some stability guarantee is required for DC/DC converters with CPLs.

In contrast to previous research, this paper introduces a one-step CCS-MPC for the output voltage in second-order DC/DC converters while supplying a CPL. The contributions of this paper are threefold:

- An analysis of the instability of second-order DC/DC converters when supplying a CPL in an open loop is presented in discrete time via the triangle criterion. Although the instability of CPLs has been previously reported, the use of this criterion constitutes a simple and pedagogical way to understand the phenomenon.
- A one-step CCS-MPC approach is proposed to regulate the output voltage in second-order DC/DC converters. The optimization problem is analyzed in detail with a closed-form control that is easily implementable.
- The conditions for stability in closed-loop operation are formally found, showing a remarkably high performance. These conditions can be transformed into a convex optimization problem that can be solved during the design process. A simulation-based approach is proposed to validate the effectiveness of our proposal.

The rest of this paper is organized as follows. Section 2 presents a generalized nonlinear discrete-time dynamic system for DC/DC converters with CPLs. Additionally, this section analyzes the stability of the converter in open-loop operation, and it outlines our CCS-MPC-based proposal. Finally, this section analyzes stability in a closed loop. Section 3 presents the simulation results of the proposed control, and the main findings of this paper are listed in Section 4.

Notation. Functions and vector fields are assumed to be smooth over the respective definition spaces. $\mathbb{R}$ denotes the set of real numbers. Matrices are represented by capital letters. Vectors and scalars are represented by lowercase letters, as well as entries of the matrices. Thus, a matrix $G \in \mathbb{R} \times \mathbb{R}$ has entries g_{ij}. For any vector $x \in \mathbb{R}^n$, $\|x\|$ is the Euclidean norm, and $\|x\|_Q$ is $\sqrt{x^\top Q x}$ with $Q \succ 0$. The symbols $\succeq$ and $\succ$ represent semi-definite and definite conditions, respectively. $\otimes$ represents the Kronecker product of two matrices.

2. Dynamic analysis and proposed control for DC/DC converters

2.1. Discrete-time model for DC/DC converters

This work considers second-order DC/DC converters of the Buck, Boost, Buck-Boost, and non-inverting Buck-Boost type feeding a CPL,

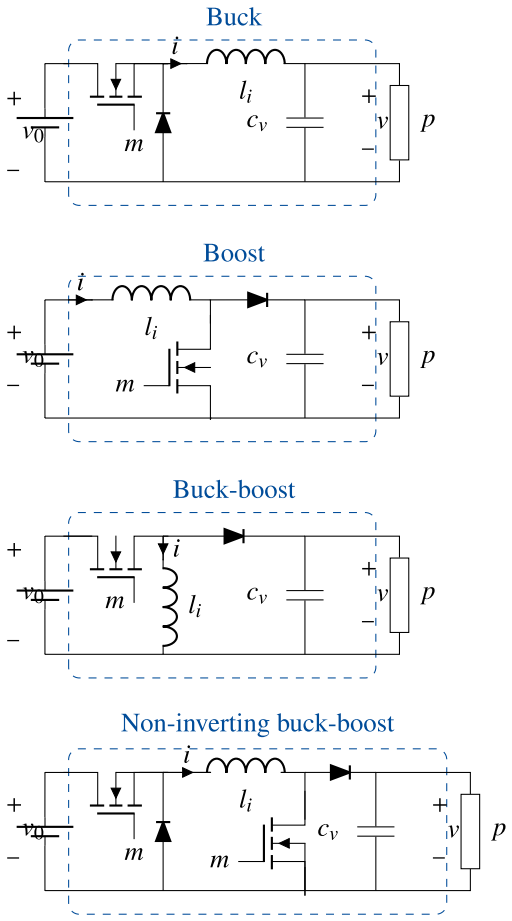

Fig. 1. Configuration of different DC/DC converters feeding a CPL with $p \geq 0$: a) Buck converter, b) Boost converter, c) Buck-Boost converter, d) non-inverting Buck-Boost converter.

as depicted in Fig. 1. The following generalized nonlinear discrete-time dynamic system can represent these converters:

$$x^+ = M^{-1}\left(A(x)x + (\xi_1 + \xi_2 u)Bx + (\xi_3 + \xi_4 u)b\right), \tag{1}$$

with states $x = (i, v)$ and input u (*i.e.*, the modulation index); M, $A(x)$, and B are 2×2 matrices given below:

$$M = \begin{bmatrix} \alpha_l & 0 \\ 0 & \alpha_c \end{bmatrix},$$
$$A(x) = \begin{bmatrix} \alpha_l & 0 \\ 0 & \alpha_c - p/x_2^2 \end{bmatrix}, \tag{2}$$
$$B = \begin{bmatrix} 0 & -1 \\ 1 & 0 \end{bmatrix}.$$

Constants α are given by $\alpha_l = l_i/\tau$ and $\alpha_c = c_v/\tau$, where τ is the discretization time. These constants are evident in Fig. 1. Without compromising generality, it is assumed that $x_2 \neq 0$ and $p > 0$. Finally, $b = [v_0, 0]^\top$ and ξ_i are vectors given in Table 1.

In this model, the vector of states x belongs to the set of positive real numbers, except for the voltage of the Buck-Boost converter, which is $v < 0$. Moreover, the supply voltage for the DC/DC converters is greater than zero ($v_0 > 0$), as are the parameters (capacitance and inductance) of the DC/DC converters (c_v, $l_i > 0$). It is common practice for DC/DC converters to impose a modulation index in open-loop operation to feed a general load. However, this is not an option in the case of CPLs, since the equilibrium point is unstable for a constant modulation index, as is proven in the next section.

Table 1
General representation of the Buck, Boost, Buck-Boost and non-inverting Buck-Boost converters.

Converter	ξ_1	ξ_2	ξ_3	ξ_4
Buck	1	0	0	1
Boost	1	-1	1	0
Buck-Boost	-1	1	0	1
Non-inverting Buck-Boost	1	-1	0	1

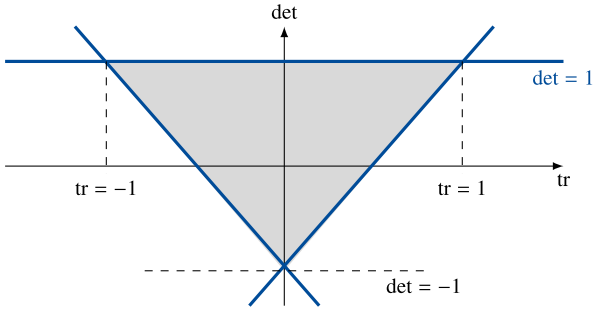

Fig. 2. Criterion for the stability of a discrete dynamic system in $\mathbb{R}^2$. Only the area inside the shaded triangle leads to a stable system.

2.2. Open-loop dynamics

The following result in $\mathbb{R}^2$ is used to study the stability of the system:

Lemma 1 *([41] pg. 200). A two-dimensional discrete-time dynamic system $\Delta x^+ = J\Delta x$ is asymptotically stable if and only if*

$$|\operatorname{tr}(J)| - 1 < \det(J) < 1. \tag{3}$$

This lemma defines a stability region by using the trace and the determinant of J without explicitly calculating its eigenvalues. Moreover, it allows determining the instability of a dynamic system. Fig. 2 depicts the criterion.

Below, the dynamics of the second-order converters and their corresponding equilibrium points are studied.

Lemma 2. *The discrete dynamic system given by (1) admits equilibrium points $(\bar{x}, \bar{u})$ in the following set:*

$$\Omega = \left\{ \begin{array}{l} 0 = (\xi_1 + \xi_2\bar{u})\bar{x}_2 - (\xi_3 + \xi_4\bar{u})v_0 \\ p = (\xi_1 + \xi_2\bar{u})\bar{x}_1\bar{x}_2 \end{array} \right\} \tag{4}$$

with $\bar{u} \neq 0$ and $\bar{x}_2 \neq 0$.

Proof. At the equilibrium point,

$$M\bar{x} = A(\bar{x})\bar{x} + (\xi_1 + \xi_2\bar{u})B\bar{x} + (\xi_3 + \xi_4\bar{u})b. \tag{5}$$

This is multiplied by $e_1^\top = [1, 0]$ to obtain the first expression and by $e_2^\top = [0, 1]$ to obtain the second expression in Ω. Note that $e_1^\top B\bar{x} = -\bar{x}_2$, $e_1^\top(M - A(\bar{x}))\bar{x} = 0$, $e_2^\top(M - A(\bar{x}))\bar{x} = p/\bar{x}_2$, and $e_1^\top b = v_0$. □

Now, the first result regarding the stability of the open-loop system can be presented:

Theorem 1. *Every equilibrium point $\bar{x} \in \Omega$ of (1) is open-loop unstable.*

Proof. The linearization of (1) for a constant input $u = \bar{u}$ is formulated, where the Jacobian matrix J_0 is calculated as presented below:

$$J_0 = M^{-1}\left(J_A + J_B\right), \tag{6}$$

where

$$J_A = \begin{bmatrix} \alpha_l & 0 \\ 0 & \alpha_c + \frac{p}{\bar{x}_2^2} \end{bmatrix} \tag{7}$$

and

$$J_B = (\xi_1 + \xi_2 \bar{u})B. \tag{8}$$

The determinant of J_0 is given below:

$$\det(J_0) = \det(M^{-1}(J_A + J_B)) \tag{9}$$

$$= \det(M^{-1})\det(J_A + J_B). \tag{10}$$

The following identity is valid for any pair of 2×2 matrices:

$$\det(J_A + J_B) = \det(J_A) + \det(J_B) + \mathrm{tr}(J_A)\mathrm{tr}(J_B) - \mathrm{tr}(J_A J_B). \tag{11}$$

Moreover, the matrices J_A and J_B have the following properties:

$$\mathrm{tr}(J_A) = \alpha_l + \alpha_c + \frac{p}{\bar{x}_2^2}, \tag{12}$$

$$\mathrm{tr}(J_B) = 0, \tag{13}$$

$$\det(J_A) = \alpha_l \alpha_c + \frac{\alpha_l p}{\bar{x}_2^2}, \tag{14}$$

$$\det(J_B) = (\xi_1 + \xi_2 \bar{u})^2, \tag{15}$$

therefore,

$$\det(J_0) = \det(M^{-1})(\det(J_A) + \det(J_B)) \geq \left(\frac{1}{\alpha_l \alpha_c}\right)\left(\alpha_l \alpha_c + \frac{\alpha_l p}{\bar{x}_2^2}\right) \geq 1. \tag{16}$$

The above-presented inequality is explained by the fact that $\alpha_x > 0$, $p > 0$, and $\det(J_B) \geq 0$. Since $\det(J) = \lambda_1 \lambda_2$ with $\lambda = \mathrm{eig}(J_0)$, it can be concluded that at least one eigenvalue is outside the unit circle. In addition, due to Lemma 1, the system is open-loop unstable. □

Remark 1. The instability of the CPLs has been previously studied using different approaches. However, to the best of the authors' knowledge, this is the first time that trace-determinant criteria is used to this effect. These criteria are simple and general for any DC/DC converter. This generality is relevant since the system is rendered unstable regardless of the particular parameters of the converters.

2.3. Proposed MPC

Lemma 2 clearly shows the need for a control that ensures stability. Furthermore, improving the performance of the closed-loop system is desirable. Therefore, a horizon-one CCS-MPC is proposed based on the following OCP:

$$\begin{aligned} &\min \frac{1}{2}\left\|M(x^+ - \bar{x})\right\|_Q^2 + \frac{\rho}{2}(u - \bar{u})^2 \\ &\text{s.t.} \\ &\quad M x^+ = A(x)x + (\xi_1 + \xi_2 u)Bx + (\xi_3 + \xi_4 u)b \\ &\quad u \in \mathcal{U} = \left\{u \in \mathbb{R} : u_{\min} \leq u \leq u_{\max}\right\} \end{aligned} \tag{17}$$

with $Q \succ 0$, $\rho > 0$, $u_{\min} > 0$, and $u_{\max} \leq 1$. Solving this OCP yields the following control law:

$$u(x) = \mathrm{proj}_{\mathcal{U}}\left(\frac{\rho\bar{u} - \psi_1(x)^\top Q \psi_2(x)}{\rho + \psi_2(x)^\top Q \psi_2(x)}\right), \tag{18}$$

with $\psi_1 : \mathbb{R}^2 \to \mathbb{R}^2$ and $\psi_2 : \mathbb{R}^2 \to \mathbb{R}^2$, given by (19) and (20), respectively:

$$\psi_1(x) = A(x)x + \xi_1 Bx + \xi_3 b - M\bar{x}, \tag{19}$$

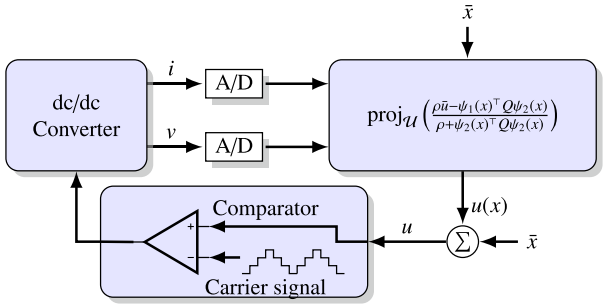

Fig. 3. Proposed horizon-one CCS-MPC for second-order DC/DC converters feeding a CPL.

$$\psi_2(x) = \xi_2 Bx + \xi_4 b. \tag{20}$$

Note that $\psi_1(\bar{x}) + \bar{u}\psi_2(\bar{x}) = 0$. Hence, $u(\bar{x}) = \bar{u}$.

This simple algebraic equation can be implemented in practice without any sophisticated optimization toolbox, as it is common in model predictive applications. The switching frequency is constant since the control action is directly applied to the modulation index (*i.e.*, it is a CCS-MPC). Fig. 3 shows the schematic representation of the control.

Lemma 3. *Equation* (18) *is the unique global minimizer of* (17).

Proof. The objective function is obviously convex – and strongly so – since M is non-singular, $Q \succ 0$, and $\rho > 0$. In addition, the equality constraints are affine, and $\mathcal{U}$ are box constants. Therefore, the optimization problem in (17) is convex and strictly convex, which implies a global optimum and a unique solution. □

In addition to these practical advantages, the proposed control has a stability guarantee, as demonstrated in the next section.

2.4. Closed-loop stability

The linearized model of the closed-loop system is required in order to study the stability of the MPC given by (18). Hence, the Jacobian matrix for the closed-loop system is calculated with $\bar{u} \in \mathrm{int}(\mathcal{U})$:

$$J = M^{-1}\left(J_A + J_B + J_C\right), \tag{21}$$

with $J_C = \psi_2(\bar{x})J_u^\top$, where ψ_2 is given by (20) evaluated at $\bar{x}$ and J_u is given below:

$$J_u = \left.\frac{\partial u}{\partial x}\right|_{x=\bar{x}} = -\frac{1}{\sigma}J_{AB}^\top Q \psi_2(\bar{x}). \tag{22}$$

Note that $\psi_2(x)$ and J_u are vectors in $\mathbb{R}^2$, so J_C is a matrix in $R^{2\times 2}$.

Therefore, the linearization of (1), with input $u \in \mathcal{U}$ given by (18) at the equilibrium point $\bar{x} \in \Omega$, is:

$$J = J_0 - \frac{1}{\sigma}J_M Q J_{AB}, \tag{23}$$

with

$$\sigma = \rho + \psi_2(\bar{x})^\top Q \psi_2(\bar{x}), \tag{24}$$

$$J_M = M^{-1}\psi_2(\bar{x})\psi_2(\bar{x})^\top, \tag{25}$$

$$J_{AB} = (J_A + J_B). \tag{26}$$

In these equations, J_0, J_A, and J_B, are given by (6), (7), and (8), respectively. The difference between (6) and (21) is that the latter considers the effect of the control.

Theorem 2. *The MPC* (17) *is asymptotically stable if Q and ρ are selected such that the following linear matrix inequalities hold:*

$$
\begin{aligned}
&\rho \geq 0,\\
&Q \succ 0,\\
&y_1 = \rho + \psi_2^{\top} Q \psi_2,\\
&y_2 = \mathrm{tr}(J_M Q J_{AB}),\\
&y_3 = \mathrm{tr}(J_0 J_M Q J_{AB}),\\
&(\beta_1 - 1) y_1 \leq \beta_2 y_2 - y_3,\\
&\beta_2 y_1 - y_2 \leq (1+\beta_1) y_1 - \beta_2 y_2 + y_3,\\
&\beta_2 y_1 - y_2 \geq -((1+\beta_1) y_1 - \beta_2 y_2 + y_3),
\end{aligned}
\tag{27}
$$

with the constants β_1, β_2 defined as follows:

$$\beta_1 = \det(J_0),\ \beta_2 = \mathrm{tr}(J_0). \tag{28}$$

Proof. The following result can be easily deduced from the corresponding definition:

$$\det(J_M Q J_{AB}) = 0. \tag{29}$$

The definitions of y_1, y_2, y_3 in (27) are used, as well as the identity for the determinant of a sum, to obtain the following[1]:

$$\det(J) = \beta_1 - \frac{\beta_2}{y_1} y_2 + \frac{1}{y_1} y_3. \tag{30}$$

In addition,

$$\mathrm{tr}(J) = \beta_2 - \frac{1}{y_1} y_2. \tag{31}$$

Hence, the conditions of Lemma 1 can be written in terms of y_1, y_2, and y_3. Thus, $\det(J \leq 1$ is equivalent to the following constraint:

$$(\beta_1 - 1) y_1 \leq \beta_2 y_2 - y_3. \tag{32}$$

Likewise, $|\mathrm{tr}(J)| \leq 1 + \det(J)$ is equivalent to:

$$|\beta_2 y_1 - y_2| \leq y_1 + \beta_1 y_1 - \beta_2 y_2 + y_3. \tag{33}$$

Thus, Equation (27) summarizes the same conditions as Lemma 1 to ensure the stability of the closed-loop system. □

Theorem 2 not only provides conditions for stability, but also a methodology to find the correct values of Q and ρ that ensure a stable system. There are infinite matrices that can be used, but the user can define one with optimal performance as follows:

$$
\begin{aligned}
&\min \ \ \|Q\|\\
&\text{subject to (27)},
\end{aligned}
\tag{34}
$$

where $\|\cdot\|$ denotes any matrix norm.

Other objective functions can be employed to find the values of Q. For example, maximizing y_2 or maximizing ρ are valid approaches, subject to the set of constraints (27). The approach presented in (34) shows a good numerical performance and provides geometrical intuition.

3. Results and discussion

The proposed one-step CCS-MPC was evaluated in a second-order DC/DC converter feeding a CPL. The parameters used for the converters and the control are listed in Table 2.

Initially, the converter was simulated with a constant modulation index in order to exemplify the open-loop instability phenomenon studied in Section 2.2. Afterwards, the performance of the proposed control was analyzed and complemented with a sensitivity analysis.

[1] This identity is only valid for 2×2 matrices.

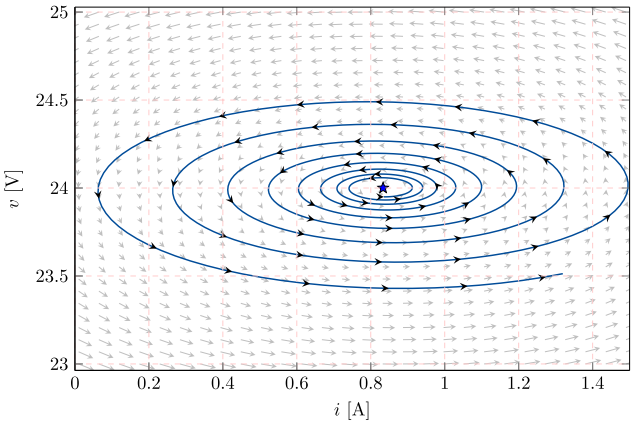

Fig. 4. Phase portrait of a Boost converter in open loop. The dynamic response is a spiral source, even for a small variation from the equilibrium.

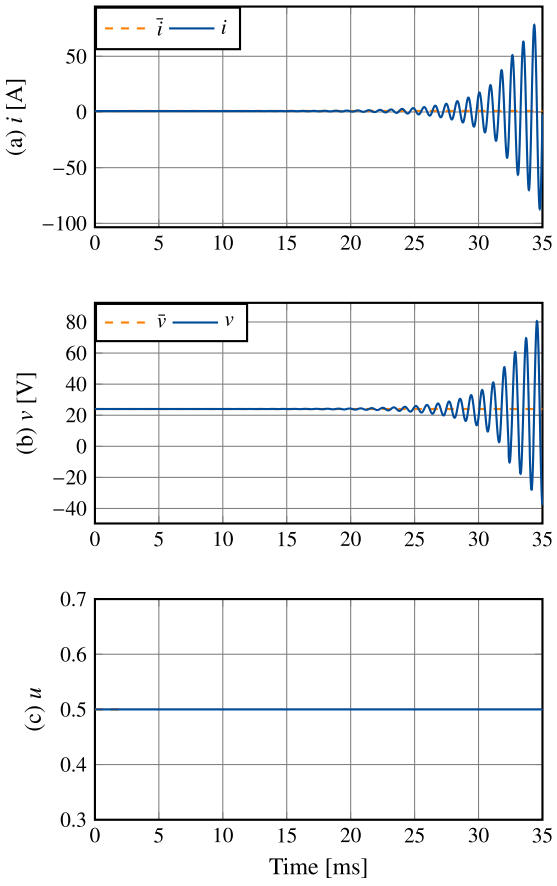

Fig. 5. Dynamic response of the Boost converter with a constant modulation index.

3.1. Open-loop instability

Consider a Boost converter in open loop that feeds a CPL. The Boost converter operates at $c_v = 100$ µF, $l_i = 47$ µH, $v_0 = 12$ V, and $v = 24$ V, connected to a $p = 10$ W with a switching frequency of 100 kHz. Fig. 4 illustrates the phase portrait of this converter in open loop. The state vector x starts at $\bar{x} = [0.83\ \text{A},\ 23.95\ \text{V}]^{\top}$ (*i.e.*, a small variation from the equilibrium). The trajectory clearly shows that the point is unstable, as expected from Theorem 1.

Fig. 5 illustrates the dynamic response of the Boost converter when the CPL changes from $p = 10$ W to $p = 10.01$ W at 2 s while the control signal remains constant, *i.e.*, a constant modulation index is applied.

Table 2
Parameters for different second-order DC/DC converters and the control.

Converter	v_0	$\bar{v}$	c_v	l_i	ρ	Q
Buck	24 V	12 V	100 µF	47 µH	27.0387	$\begin{bmatrix} 1.0546 & 0.9455 \\ 0.9455 & 1.0545 \end{bmatrix}$
Boost	12 V	24 V	100 µF	47 µH	25.1298	$\begin{bmatrix} 1.0261 & 0.9739 \\ 0.9739 & 1.0261 \end{bmatrix}$
Buck-Boost	12 V	-24 V	100 µF	47 µH	793.7977	$\begin{bmatrix} 8.6670 & -49.4975 \\ -49.4975 & 481.4370 \end{bmatrix}$
NI Buck-Boost	12 V	24 V	100 µF	47 µH	180.1889	$\begin{bmatrix} 2.1482 & 9.8425 \\ 9.8425 & 81.2510 \end{bmatrix}$

This figure shows that the Boost converter becomes unstable if the control signal remains constant and the converter experiences minimal disturbance or a change in its operating point.

It is worth adding that the performance of the other converters is similar for open-loop operation (*i.e.*, for a constant modulation index).

3.2. Performance of the proposed control

The convex optimization model given by (34) was implemented to find the values of Q and ρ for each DC/DC converter. This was done in MATLAB using the Yalmip interface [42]. Table 1 lists the values of Q and ρ, considering that all converters feed a CPL with $p = 10$ W. It is important to note that this optimization was performed off-line during design, so time is not a relevant aspect.

Fig. 6 shows the response for a Boost converter, considering that the CPL varies from $p = 10$ W to $p = 20$ W between 0.70 ms and 1.40 ms. Fig. 6a presents the current through the inductor and its reference, while Fig. 6b illustrates the output voltage of the Boost converter as well as its reference. Fig. 6c shows the control signal.

Fig. 6b evidences that the proposed control can regulate the output voltage of the Boost converter under CPL variations and stabilize it in less than 0.2 ms. Furthermore, the output voltage shows deviations of less than 0.1 V, demonstrating its excellent performance. As seen in Fig. 6c, the control signal remains stable and far from its limits, indicating that the converter operates stably and can withstand further load changes.

Fig. 7 illustrates the response of a Buck-Boost converter, considering a variable CPL ranging from $p = 10$ W to $p = 20$ W between 0.70 ms and 1.40 ms. Fig. 7a presents the current through the inductor and its reference, and Fig. 7b illustrates the output voltage of the Boost converter alongside its reference. Lastly, Fig. 7c depicts the control signal.

According to the dynamic response in Fig. 6a, the inductor current experiences an overshoot due to the sudden change in load. However, it then converges as a first-order system, which is possible because of the proposed control. When analyzing Fig. 6b, it becomes evident that the proposed control strategy adeptly regulates the output voltage of the Boost converter amidst fluctuations in a CPL, achieving stabilization in a remarkable time span of less than 0.1 ms. Additionally, the output voltage exhibits minimal deviations measuring less than 0.1 V, which demonstrates the exceptional performance of our proposal. As seen in Fig. 6c, the control signal remains stable, consistently staying within its operational limits. This observation suggests that the converter is resilient to further load variations, confirming its ability to maintain a stable operation.

In order to analyze the performance of the proposed MPC, three indices were used: the integral of the time-multiplied square-error criterion (ITSE), the integral absolute error criterion (IAE), and the integral of the time-multiplied absolute error criterion (ITAE). These indices were computed as follows:

$$\text{ITSE} = \int_0^{t_f} t\,(v(t) - \bar{v}(t))^2\,dt, \tag{35}$$

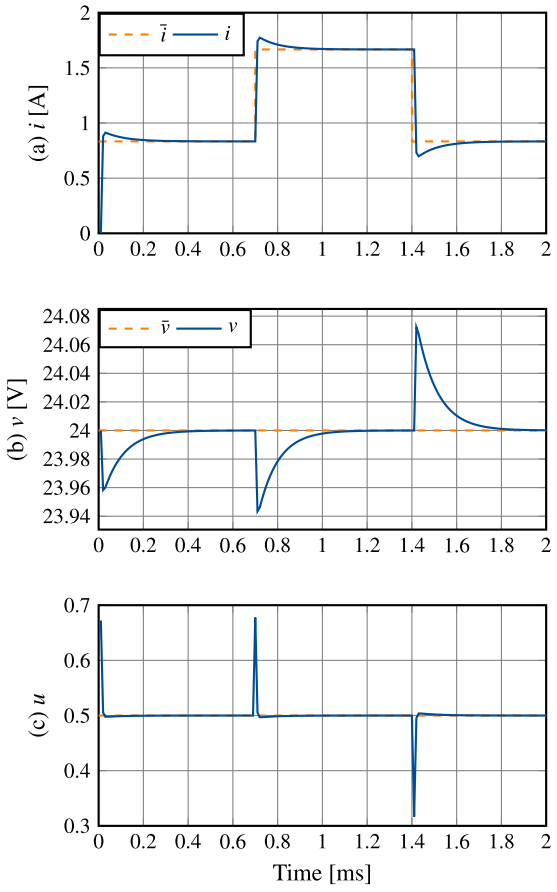

Fig. 6. Dynamic response of the Boost converter to variations in a CPL.

$$\text{IAE} = \int_0^{t_f} |v(t) - \bar{v}(t)|\,dt, \tag{36}$$

$$\text{ITAE} = \int_0^{t_f} t\,|v(t) - \bar{v}(t)|\,dt, \tag{37}$$

where t_f is the final simulation time.

Table 3 presents the values of the three indices and the settling time (T_s) regarding the output voltage for the proposed control. The results of the ITSE, with values of 4.915×10^{-6} and 3.366×10^{-6} for the Boost and Buck-Boost converters, respectively, indicate that the proposed MPC is exceptionally efficient at reducing error over time. This extremely low value suggests that the controller is highly effective at minimizing square error as time progresses, which can translate into a very precise and stable system response under dynamic conditions. The IAE values are 1.521×10^{-2} and 6.607×10^{-3} for the Boost and

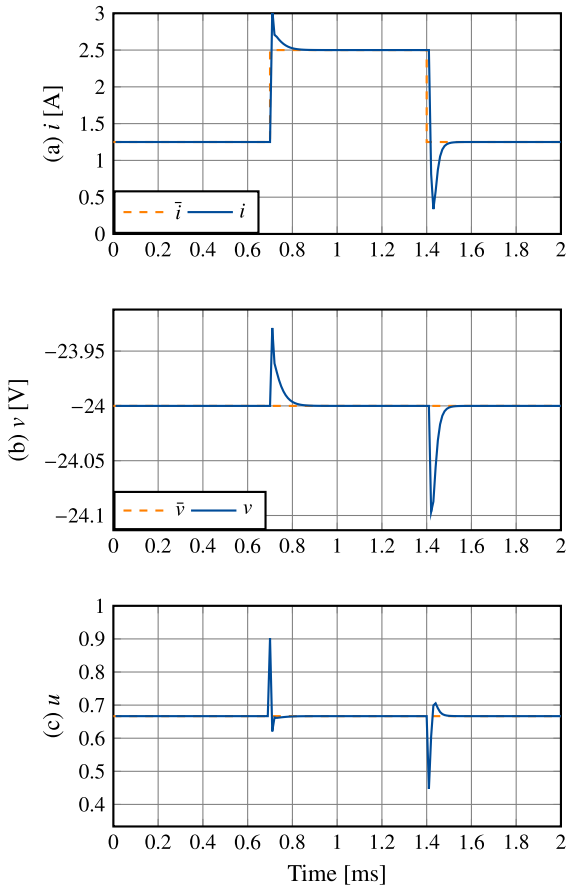

Fig. 7. Dynamic response of the Buck-Boost converter to CPL variations.

Table 3
Summary of analyzed indices.

Converter	ITSE	IAE	ITAE	T_s [ms]
Boost	4.915×10^{-6}	1.521×10^{-2}	1.521×10^{-4}	5
Buck-Boost	3.366×10^{-6}	6.607×10^{-3}	6.608×10^{-5}	1.5

Buck-Boost converters. These values consider both the magnitude and the duration of the errors. Although they are higher than those of the ITSE, they are still relatively low. This indicates that, on average, the controller maintains errors at acceptable levels, even though there may be larger fluctuations at times. Finally, the ITAE values are extremely low in both converters, indicating that the proposed MPC offers a very rapid and accurate response, minimizing the error and response times of the converter's output voltage. This is supported by the voltage regulation settling time, which is less than 5 ms for the Boost converter and 1.5 ms for the Buck-Boost converter.

It is important to mention that, for the sake of simplicity, the same analysis is not presented for the other converters, as they showed a similar performance.

3.3. Sensitivity analysis

A common criticism of MPC for power electronic applications is the absence of a small-signal model that can be utilized for sensitivity analysis. The proposed approach introduces a linearized model (Equation (21)), which can be utilized to this effect. In order to analyze the effect of varying the CPL on the proposed MPC, the eigenvalues of the system in open- and closed-loop operation are shown when the CPL varies from 0 W to 100 W in steps of 2.5 W. Fig. 8 illustrates the movement of the eigenvalues as the power of the CPL varies from zero to 100 W for both the Booster and Buck-Boost converter.

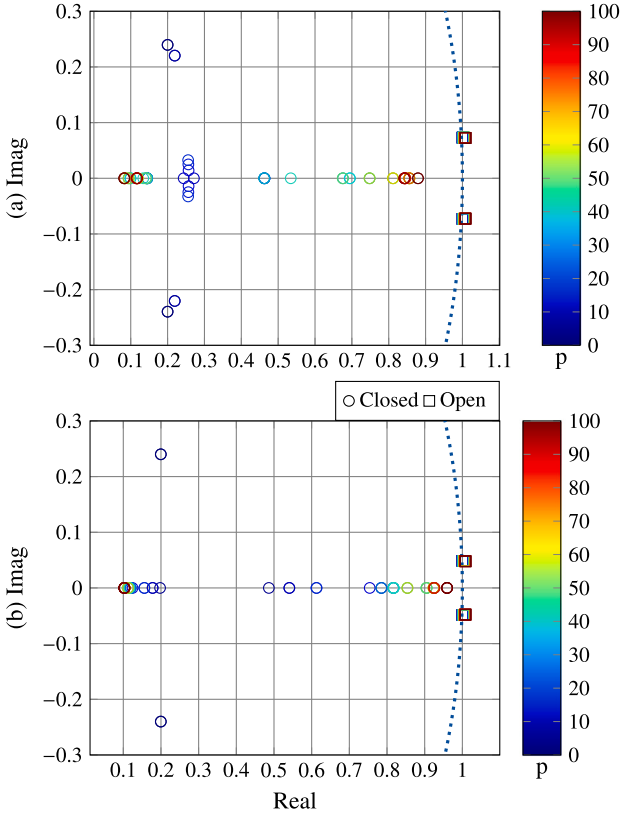

Fig. 8. Variations in the eigenvalues when the CPL varies from 0 W to 100 W: (a) Boost converter and (B) Buck-Boost converter. The dotted line denotes the stability limit, *i.e.*, the eigenvalue magnitude is equal to 1.

Fig. 8 shows that the behavior of the eigenvalues is similar for both converters. When the CPL has small values, the eigenvalues are composed of real and imaginary parts. On the other hand, if the CPL has values greater than 25 W, the eigenvalues only have real values. This means that their responses do not contain oscillations. However, one of them tends to 1, which represents the limit of stability of the system.

4. Conclusions

Second-order DC/DC converters experience unstable behaviors when supplying CPLs, given the negative impedance caused by the hyperbolic relationship between voltage and power in this type of load. To address these instabilities, this paper proposes an analytical approach to understanding the instability phenomena in DC/DC converters. A formal proof of this unstable behavior is presented, using the trace/determinant criterion for discrete-time nonlinear dynamic systems, which is also known as the *triangle criterion*. This approach has been shown to be a simple yet effective and formal way to study stability in second-order converters.

A one-step MPC was designed for the converters, taking a nonlinear discrete model into account. Unlike previous approaches, this control offers theoretical guarantees, such as the stability and global optimality of the nonlinear optimization problem. The proposed analysis is general for Buck, Boost, Buck-Boost, and non-inverting Buck-Boost converters, which have a similar mathematical structure.

Numerical simulations in the Boost and Buck-Boost converters showed stabilization times of about 5 ms and 1.5 ms. In addition, the performance indicators (IAE, ITAE, and ITSE) showed values between 1.521×10^{-2} and $4.591 \times 10^{-}6$ for the Boost converter and between

6.607×10^{-3} and 3.366×10^{-6} for the Buck-Boost topology. These numerical data confirm the effectiveness of the proposed one-step MPC approach regarding voltage regulation while considering variations in CPLs.

A sensitivity analysis of the eigenvalues of the Buck and Boost converters supplying CPLs with power variations from 0 W to 100 W revealed that the proposed controller ensures closed-loop stability under all the load conditions examined. The proposed control demonstrated a remarkable stability performance both in theory and in practice. Simulations considering the open-loop calculation of the control input at the equilibrium point confirmed that the presence of CPLs with small perturbations causes the voltage and current variables to become unstable, highlighting the significance of implementing control strategies, such as the one-step MPC approach, to address these instabilities.

Both the stability conditions and the sensitivity analysis are easy to consider in the design stage in order to obtain suitable values of Q and ρ in the objective function. Thus, the proposed framework goes beyond analysis as a practical tool for designing control systems.

Further research could include (i) extending the proposed one-step MPC approach to converters for the integration of renewable sources or energy storage systems in AC networks, such as voltage- or current-source converters; (ii) incorporating uncertainties related to control converter parameters in the proposed approach; and (iii) exploring estimators for the voltage input and the CPL connected to DC/DC converters.

CRediT authorship contribution statement

Alejandro Garcés-Ruiz: Writing – review & editing, Writing – original draft, Software, Resources, Methodology, Investigation, Conceptualization. **Walter Gil-González:** Writing – review & editing, Validation, Software, Methodology, Investigation, Funding acquisition, Formal analysis. **Oscar Danilo Montoya:** Writing – review & editing, Supervision, Software, Methodology, Investigation, Formal analysis, Conceptualization.

Declaration of competing interest

The authors declare that they have no known competing financial interests or personal relationships that could have appeared to influence the work reported in this paper.

Data availability

No data was used for the research described in the article.

Acknowledgements

This work was partially supported by the project 6-24-2 by Universidad Tecnológica de Pereira's Vicerrectoría de Investigaciones, Innovación y Extensión [Vice-Principalship for Research Innovation, and Extension]. The authors are also grateful for the financial support from the Electrical Engineering graduate and undergraduate Programs of la Universidad Tecnológica de Pereira (Colombia).

References

[1] T.K. Gimenes, M.P.C.d. Silva, J.J.G. Ledesma, O.H. Ando, Impact of distributed energy resources on power quality: Brazilian scenario analysis, Electr. Power Syst. Res. 211 (2022) 108249, https://doi.org/10.1016/j.epsr.2022.108249.

[2] S. Panda, S. Mohanty, P.K. Rout, B.K. Sahu, S.M. Parida, H. Kotb, A. Flah, M. Tostado-Véliz, B. Abdul Samad, M. Shouran, An insight into the integration of distributed energy resources and energy storage systems with smart distribution networks using demand-side management, Appl. Sci. 12 (17) (2022) 8914, https://doi.org/10.3390/app12178914.

[3] D. Infield, P. Onions, A. Simmons, G. Smith, Power quality from multiple grid-connected single-phase inverters, IEEE Trans. Power Deliv. 19 (4) (2004) 1983–1989, https://doi.org/10.1109/tpwrd.2004.829950.

[4] P. Nithara, M. Chithra, R.P. Eldho, S. Michail, Review on role of power electronics in integration of renewable energy sources with micro grid, in: 2022 International Conference on Smart and Sustainable Technologies in Energy and Power Sectors (SSTEPS), IEEE, 2022, pp. 27–32.

[5] S. Alghamdi, H.F. Sindi, A. Al-Durra, A.A. Alhussainy, M. Rawa, H. Kotb, K.M. AboRas, Reduction in voltage harmonics of parallel inverters based on robust droop controller in islanded microgrid, Mathematics 11 (1) (2022) 172, https://doi.org/10.3390/math11010172.

[6] L.I. Minchala-Avila, L.E. Garza-Castañón, A. Vargas-Martínez, Y. Zhang, A review of optimal control techniques applied to the energy management and control of microgrids, Proc. Comput. Sci. 52 (2015) 780–787, https://doi.org/10.1016/j.procs.2015.05.133.

[7] F. Ni, Z. Zheng, Q. Xie, X. Xiao, Y. Zong, C. Huang, Enhancing resilience of dc microgrids with model predictive control based hybrid energy storage system, Int. J. Electr. Power Energy Syst. 128 (2021) 106738, https://doi.org/10.1016/j.ijepes.2020.106738.

[8] M. Schwenzer, M. Ay, T. Bergs, D. Abel, Review on model predictive control: an engineering perspective, Int. J. Adv. Manuf. Technol. 117 (5) (2021) 1327–1349, https://doi.org/10.1007/s00170-021-07682-3.

[9] A. Marahatta, Y. Rajbhandari, A. Shrestha, S. Phuyal, A. Thapa, P. Korba, Model predictive control of dc/dc boost converter with reinforcement learning, Heliyon 8 (11) (2022) e11416, https://doi.org/10.1016/j.heliyon.2022.e11416.

[10] M.M. Aghdam, L. Li, J. Zhu, Comprehensive study of finite control set model predictive control algorithms for power converter control in microgrids, IET Smart Grid 3 (1) (2020) 1–10, https://doi.org/10.1049/iet-stg.2018.0237.

[11] M. Schwenzer, M. Ay, T. Bergs, D. Abel, Review on model predictive control: an engineering perspective, Int. J. Adv. Manuf. Technol. 117 (5–6) (2021) 1327–1349, https://doi.org/10.1007/s00170-021-07682-3.

[12] A. Domina, V. Tihanyi, Model predictive controller approach for automated vehicle's path tracking, Sensors 23 (15) (2023) 6862, https://doi.org/10.3390/s23156862.

[13] M.A. Santos, A. Ferramosca, G.V. Raffo, Nonlinear model predictive control schemes for obstacle avoidance, J. Control Autom. Electr. Syst. 34 (5) (2023) 891–906, https://doi.org/10.1007/s40313-023-01024-2.

[14] A. AlAttar, D. Chappell, P. Kormushev, Kinematic-model-free predictive control for robotic manipulator target reaching with obstacle avoidance, Front. Robot. AI 9 (Feb. 2022), https://doi.org/10.3389/frobt.2022.809114.

[15] A. Aouaichia, K. Kara, M. Benrabah, M.L. Hadjili, Constrained neural network model predictive controller based on Archimedes optimization algorithm with application to robot manipulators, J. Control Autom. Electr. Syst. 34 (6) (2023) 1159–1178, https://doi.org/10.1007/s40313-023-01033-1.

[16] K. Salahshoor, M.H. Asheri, M. Hadian, M. Doostinia, M. Babaei, A novel exergy-based optimization approach in model predictive control for energy-saving assessment, J. Control Autom. Electr. Syst. 31 (6) (2020) 1481–1488, https://doi.org/10.1007/s40313-020-00640-6.

[17] S. Vazquez, J.I. Leon, L.G. Franquelo, J. Rodriguez, H.A. Young, A. Marquez, P. Zanchetta, Model predictive control: a review of its applications in power electronics, IEEE Ind. Electron. Mag. 8 (1) (2014) 16–31, https://doi.org/10.1109/mie.2013.2290138.

[18] K.V. Konneh, O.B. Adewuyi, M.E. Lotfy, Y. Sun, T. Senjyu, Application strategies of model predictive control for the design and operations of renewable energy-based microgrid: a survey, Electronics 11 (4) (2022) 554, https://doi.org/10.3390/electronics11040554.

[19] S. Vazquez, J. Rodriguez, M. Rivera, L.G. Franquelo, M. Norambuena, Model predictive control for power converters and drives: advances and trends, IEEE Trans. Ind. Electron. 64 (2) (2017) 935–947, https://doi.org/10.1109/tie.2016.2625238.

[20] S. Kouro, P. Cortes, R. Vargas, U. Ammann, J. Rodriguez, Model predictive control—a simple and powerful method to control power converters, IEEE Trans. Ind. Electron. 56 (6) (2009) 1826–1838, https://doi.org/10.1109/tie.2008.2008349.

[21] M. Abdelrahem, J. Rodríguez, R. Kennel, Improved direct model predictive control for grid-connected power converters, Energies 13 (10) (2020) 2597, https://doi.org/10.3390/en13102597.

[22] S. Gros, M. Zanon, Learning for mpc with stability & safety guarantees, Automatica 146 (2022) 110598, https://doi.org/10.1016/j.automatica.2022.110598.

[23] D. Mayne, J. Rawlings, C. Rao, P. Scokaert, Constrained model predictive control: stability and optimality, Automatica 36 (6) (2000) 789–814, https://doi.org/10.1016/S0005-1098(99)00214-9, https://www.sciencedirect.com/science/article/pii/S0005109899002149.

[24] A. Garcés, Stability analysis of dc-microgrids: a gradient formulation, J. Control Autom. Electr. Syst. 30 (6) (2019) 985–993, https://doi.org/10.1007/s40313-019-00525-3.

[25] S.A.G.K. Abadi, S.I. Habibi, T. Khalili, A. Bidram, A model predictive control strategy for performance improvement of hybrid energy storage systems in DC microgrids, IEEE Access 10 (2022) 25400–25421.

[26] M.E. Albira, M.A. Zohdy, Adaptive model predictive control for DC-DC power converters with parameters' uncertainties, IEEE Access 9 (2021) 135121–135131.

[27] W. Gil-González, O.D. Montoya, C. Restrepo, J.C. Hernández, Sensorless adaptive voltage control for classical DC-DC converters feeding unknown loads: a generalized PI passivity-based approach, Sensors 21 (19) (2021) 6367.

[28] Y. Gui, R. Han, J.M. Guerrero, J.C. Vasquez, B. Wei, W. Kim, Large-signal stability improvement of DC-DC converters in DC microgrid, IEEE Trans. Energy Convers. 36 (3) (2021) 2534–2544.

[29] W. Du, K. Zheng, H. Wang, Oscillation instability of a DC microgrid caused by aggregation of same CPLs in parallel connection, IET Gener. Transm. Distrib. 13 (13) (2019) 2637–2645, https://doi.org/10.1049/iet-gtd.2018.6940.

[30] A.M. Abdurraqeeb, A.A. Al-Shamma'a, A. Alkuhayli, M. Alharbi, H.M.H. Farh, F. Alsaif, H.O. Omotoso, K.E. Addoweesh, A. Qamar, Stabilization of constant power loads and dynamic current sharing in DC microgrid using robust control technique, Electr. Power Syst. Res. 230 (2024) 110258.

[31] P. Karamanakos, T. Geyer, S. Manias, Direct voltage control of DC–DC boost converters using enumeration-based model predictive control, IEEE Trans. Power Electron. 29 (2) (2013) 968–978.

[32] A.J.S. Filho, R.S. Inomoto, L.L. Rodrigues, R.B.A. Cunha, O.A.C. Vilcanqui, Predictive control applied to a boost converter of a photovoltaic system, J. Control Autom. Electr. Syst. 33 (2) (2022) 393–405, https://doi.org/10.1007/s40313-021-00796-9.

[33] L.A. Maccari Jr., D.M. Lima, G.G. Koch, V.F. Montagner, Robust model predictive controller applied to three-phase grid-connected lcl filters, J. Control Autom. Electr. Syst. 31 (2) (2020) 447–460, https://doi.org/10.1007/s40313-019-00546-y.

[34] A.A. Ahmed, B.K. Koh, Y.I. Lee, A comparison of finite control set and continuous control set model predictive control schemes for speed control of induction motors, IEEE Trans. Ind. Inform. 14 (4) (2017) 1334–1346.

[35] I. Hammoud, S. Hentzelt, K. Xu, T. Oehlschlägel, M. Abdelrahem, C. Hackl, R. Kennel, On continuous-set model predictive control of permanent magnet synchronous machines, IEEE Trans. Power Electron. 37 (9) (2022) 10360–10371.

[36] C.S. Lim, S.S. Lee, E. Levi, Continuous-control-set model predictive current control of asymmetrical six-phase drives considering system nonidealities, IEEE Trans. Ind. Electron. 70 (8) (2022) 7615–7626.

[37] Y. Yang, Y. Xiao, M. Fan, K. Wang, X. Zhang, J. Hu, G. Fang, W. Zeng, S. Vazquez, J. Rodriguez, A novel continuous control set model predictive control for LC-filtered three-phase four-wire three-level voltage-source inverter, IEEE Trans. Power Electron. 38 (4) (2023) 4572–4584.

[38] B. Ren, Y. Zhu, X. Sun, Z. Pan, W. Zhao, Dynamic performance improvement of continuous control set model predictive control for high-frequency link matrix converter, IEEE Trans. Ind. Electron. 70 (9) (2022) 9057–9066.

[39] H. Javaheri Fard, S.M. Sadeghzadeh, Predictive and average current controllers for a high step-up interleaved dc–dc converter, J. Control Autom. Electr. Syst. 33 (6) (2022) 1829–1839, https://doi.org/10.1007/s40313-022-00927-w.

[40] A. Garcés-Ruiz, S. Riffo, C. González-Castaño, C. Restrepo, Model predictive control with stability guarantee for second-order DC/DC converters, IEEE Trans. Ind. Electron. 71 (5) (2024) 5157–5165.

[41] S.N. Elaydi, Discrete Chaos with Applications in Science and Engineering, CRC Press Taylor and Francis Group, London, 2007.

[42] J. Lofberg, YALMIP: a toolbox for modeling and optimization in MATLAB, in: 2004 IEEE International Conference on Robotics and Automation (IEEE Cat. No. 04CH37508), IEEE, 2004, pp. 284–289.